2.A.1 *Nuclear Physics* **69** (1965) 536—544; © *North-Holland Publishing Co., Amsterdam*

PROTON REACTION CROSS SECTIONS AT 8.8 MeV

P. J. BULMAN, G. W. GREENLEES † and M. J. SAMETBAND ††

Department of Physics, University of Birmingham, England

Received 5 December 1964

Abstract: Proton reaction cross sections at 8.8 MeV are given for Al, V, Fe, Co, Ni^{58}, Ni^{60}, Cu^{63}, Cu^{65}, Cu, Zn and Ga. An anticoincidence technique was used and the results are discussed in terms of optical model predictions.

E NUCLEAR REACTIONS ^{27}Al, V, Fe, ^{59}Co, $^{58, 60}$Ni, $^{63, 65}$Cu, Cu, Zn, Ga(p), $E = 8.8$ MeV; measured σ_{removal}; deduced $\sigma_{\text{non-elastic reaction}}$.

1. Introduction

The elastic scattering of protons in the 10 MeV region has been extensively studied by a number of workers. These measurements include both differential cross sections and polarization data and are, in general, well represented by an optical model description of the nucleus. This model provides values for the total reaction cross section σ_R, but the measurement of this quantity presents many problems near 10 MeV. Several methods have been used, often giving conflicting results. The sensitivity of the model parameters to the reaction cross section has been studied [1, 2]) and it is clear that accurate values would help to limit the volume in parameter space leading to satisfactory fits of the differential cross section and polarization data.

Early measurements [3, 4]) of σ_R for Cu at about 10 MeV gave values higher than anticipated on the basis of a volume absorptive potential and supported the suggestion that a surface form was needed. Subsequent measurements by Chackett [7]) and Carlson [8]) agreed with the earlier values but the values of Albert and Hansen [9]) Wing and Huizenga [10]) Wilkins and Igo [11]) and Bearpark [12]) indicated a lower figure. When the present experiment was started, many of these results were not available and its object was to improve the accuracy of the early data and extend the range of elements studied.

2. Method

The simple "target in", "target out" attenuation method used for neutron work is not directly applicable for protons below $\approx$ 100 MeV since ionization loss necessitates the use of thin targets which consequently give small attenuations. The anti-

† Present address: University of Minnesota, Minneapolis, USA.

†† Present address: Comision Nacional de Energia Atomica, Argentina.

coincidence attenuation technique was developed for proton work. Unfortunately, the difficulties of this method increase rapidly as the energy is reduced – approximately as the inverse square – and there was a delay of several years before it was applied around 10 MeV; during this period several other techniques were developed. The most widely applied was the indirect method of Meyer and Hintz [3]). They summed the partial cross sections by measuring the total cross section for charged particle production $\sigma(p, q)$ and adding to this the published (p, n) cross sections; the data on (p, γ) cross sections indicated that these could be neglected. More recent measurements of the (p, n) cross sections [9, 10]) have reduced the value of σ_R obtained from the $\sigma(p, q)$ measurements.

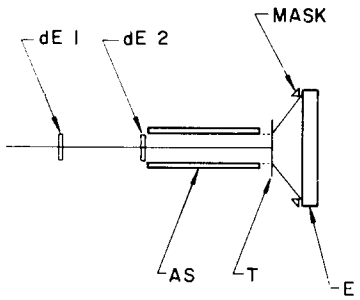

Fig. 1. The anticoincidence system. The beam enters at the left on the axis shown. The mask defines the acceptance cone for the stopping counter.

Greenlees and Jarvis [4]) used a target in, target out technique in which a rapid alternation was used to average out beam fluctuations. The main difficulty with this method was statistical; the attenuation was only 2×10^{-4} and very long counting periods were necessary. Recently Bearpark [12]) has used a charge measuring technique in which the charge collected by the target in an insulated enclosure is compared with the charge of the beam.

The anticoincidence attenuation technique has been used near 10 MeV by Carlson [8]), Wilkins and Igo [11]) and in the present work. The basic arrangement is shown in fig. 1. The incident beam is recorded by two or more passing counters dE which operate in fast coincidence and an antiscattering counter AS, in anticoincidence, is used to reject most of the protons scattered from the beam axis by the last passing counter. The target T is placed close behind the antiscattering counter and a mask is used to define the acceptance cone for the stopping counter E. In the notation of fig. 1 a count dE1 dE2 $\overline{\text{AS}}$ (where $\overline{\ }$ indicates anticoincidence) represents an incident particle and dE1 dE2 $\overline{\text{AS}}$ $\overline{\text{E}}$ is a beam loss count. It is usual to put an energy threshold on the stopping counter to discriminate against reduced energy protons.

The loss counts may arise in various ways. Typical figures for the fractional loss caused by different processes are given below for a 20 mg · cm^{-2} target of Cu.

(i) Reactions in the target: 1.5×10^{-4}

(ii) Elastic scattering in the target clear of the stopping counter and antiscattering counter: 4×10^{-5}

(iii) Reactions in the stopping counter producing pulses below a bias level of 53 % of the full energy: 4×10^{-4}

(iv) Reactions in the antiscattering counter producing pulses below its bias level. This depends critically on geometry and threshold. Present equipment gave: 2×10^{-5}

(v) Back scattering in the second passing counter: 2×10^{-5}

(vi) Back scattering from the front face of stopping counter for a bias level of 2 % of full energy: 3×10^{-5}

(vii) Reactions in the passing counters giving low energy contamination of the beam: 10^{-6}

(viii) Low-energy (less than 53 % of the full energy) contamination in the incident beam. This is very dependent on the collimation system. up to 10^{-3}

The background effects (iii)–(viii) can, in principle, be measured during a target out run. However, the reactions in the stopping counter are energy dependent and the energy must be adjusted to compensate for the energy loss in the target. This is usually done by placing a dummy absorber before the counter system. Such a procedure reduces the energy of the beam incident on all the defining counters and effects (iv)–(vii) may be altered. Insertion of a dummy may also change the geometry of the beam and the low-energy contamination caused by the collimation system; this can be a very large effect.

3. Apparatus

A schematic diagram of the arrangement used in the present work is given in fig. 2. An extracted beam of about 1 μA of 9.8 MeV protons was defined by a 1 mm hole in stop 1, passed the dummy position D, through quadrupoles Q1 and guiding coils G, to the 1 mm collimating holes 2 and 3. About 10^5 protons per second were transmitted by this system and no stops in the beam path were used after stop 3. The bending magnet deflected the beam and separated the low-energy components; the quadrupoles Q2 produced a 2.25 mm spot at dE1. The wall baffles between the magnet and dE1 were 2 cm in diam. and stops 1 cm in diam. B1, B2 were placed in front of both dE1 and dE2.

The passing counters played an important part in the final definition of the beam. Counter dE1 consisted of a piece of plastic scintillator 25 μm thick and 2.25 mm in diam. held on the beam axis by means of a Melinex foil 6 μm thick. The second passing counter dE2 was a piece of plastic scintillator 50 μm $\times$ 3.75 mm diam. mounted on an aluminium foil 0.26 mg $\cdot$ cm^{-2} placed just inside the first scintillation aperture of the antiscattering counter (see fig. 3). Light from the scintillators

of dE1 and dE2 was collected on photocathodes via reflecting cavities. In order to be regarded as incident, a proton had to pass through both passing counters. This requirement, together with the focussing of Q2, enforced a very strict geometry on the incident particles; at least two deflections were required if a proton, striking a baffle, was to be regarded as incident. The most favourable case for such a spurious

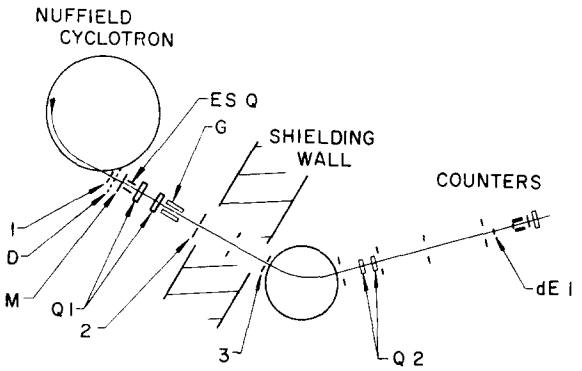

Fig. 2. Beam transport system. The beam is defined by the collimators 2 and 3 and any low-energy components are rejected by the bending magnet. The quadrupoles Q2 focus the beam to a 2.25 mm spot at dE1. The figure is not to scale; the distance from the cyclotron to the bending magnet is approximately 6 m and from the bending magnet to the counters 3 m.

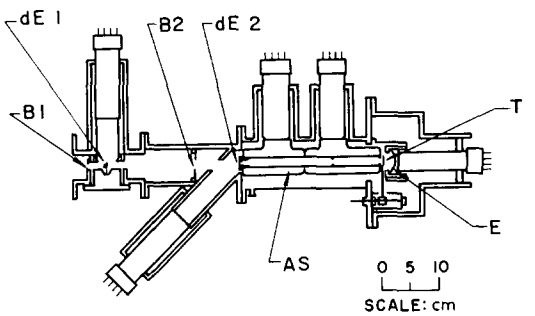

Fig. 3. Counters and target. Useful incident particles pass through the counters dE1 and dE2 and along the axis of the antiscattering counter, AS onto the target T. The stopping counter E records those not interacting in the target.

incident particle is via the baffle B2 between the two passing counters; the probability of such an event was estimated at less than 10^{-9}.

Placing the dummy before the bending magnet required that the magnetic field be changed each time the dummy was put in or out of the beam. The magnetic field was stabilized by a nuclear magnetic resonance device and changing the field required 6 sec. The switching was done automatically in step with the target and dummy changes and each channel had an open period of about 25 sec.

The arrangement described was developed following the unsatisfactory performance of a system in which the dummy and a collimator were placed after the bending magnet. In this earlier arrangement, it was impossible to reduce the low-energy contamination of the beam to acceptable proportions.

The basic radio frequency structure of the beam is 10 MHz. The electronics was capable of resolving particles accelerated on successive r.f. pulses but not particles accelerated within any one pulses. The spectrum of pulse heights from the stopping counter indicated that, for certain machine conditions, the incidence of more than one proton during one r.f. pulse occurred much more often than predicted by random distribution.

This effect was reduced to less than 1 % by means of a Melinex foil 0.1 mm thick, placed at position M (fig. 2), which increased the disorder of the beam.

Beam structure was also observed at 50, 100 and 300 Hz due to mains ripple on various D.C. supplies. The magnitude of these components could be controlled to some extent by the machine operators, and a duty cycle of 50 % could be achieved comparatively easily.

The insertion of the dummy had the effect of reducing the counting rate by a factor 30. To equalize the rate for the two dummy positions, electrostatic quadrupoles (ESQ fig. 2) were used to defocus the beam in the dummy out condition.

4. Procedure

The presence of stray and fringing magnetic fields affected the proton trajectories sufficiently to prevent the use of an optical alignment technique. The system was aligned by observing scintillator placed at various points along the beam path. The beam spot, 2.25 mm in diam., observed at dE1 and a further spot at E were stable in position over several weeks and lay accurately on the axis of the antiscattering counter.

The dummy targets were made to equalize the energy in the stopping counter as closely as possible. This sometimes resulted in a slight energy unbalance for which a small correction was necessary. Before and after each run the target position was checked and in no case was any significant shift found.

The energy of the protons incident upon the beam defining counters was different in the two conditions dummy in and out. This produced a slight change in the behaviour of the dE1 dE2 AS system. Such changes were impossible to calculate and were measured by setting the bias on the stopping counter at 2 %, holding the target out, and measuring the anticoincidence ratios for dummy in and out positions. A 2 % bias setting on the stopping counter ensured that no counts were lost due to reactions in its plastic scintillator since protons inelastically scattered to the 4.4 and 7.6 MeV levels of C^{12} would still be recorded. These account for almost all the reaction cross section [13]), the (p, n) threshold being about 18 MeV. The only incident protons not recorded would be those scattered at large angles from the front face

of the scintillator. With a bias level of 2 % this should give an anticoincidence ratio of about $3 \cdot 10^{-5}$ and similar scattering at the second passing counter adds about $2 \cdot 10^{-5}$. These estimates agree well with the observed ratios of $5 \cdot 10^{-5}$ for dummy out and $8 \cdot 10^{-5}$ for dummy in. The difference between these figures for out and in is interpreted as due to the effect of the energy change of the protons on the defining counters; changes in the scattering from carbon with energy in this region are very small.

The counting sequence was to measure the energy effect on the defining counter by the above method for 40 min, and then alternate the target and dummy for 3 h. This procedure was repeated for a total of about 20 h to achieve errors of 3–4 %. The useful counting rate (dE1 dE2 $\overline{\text{AS}}$) was about 4×10^3 per sec.

TABLE 1

Experimental reaction cross sections, showing the magnitudes of the various correction terms

Target	Energy at target centre (MeV)	Stopping counter energy bias %	Raw cross section (mb)	Elastic scattering corr. mb (subtract)	Inelastic scattering corr. mb (add)	Beam spot size corr. mb (subtract)	Reaction cross section $\sigma_R - \sigma_{CE}$ (mb)	Optical model prediction σ_R (mb)
Al	8.8	53	642±20	120±10	156±40	4±3	674±45	682
V	8.8	53	820±20	125±20	40± 5	5±3	730±30	816
Fe	8.9	70	767±40	185±20	103±26	5±3	680±50	775
Co	8.8	53	920±30	205±20	100±20	5±3	825±40	766
Ni^{58}	8.8	70	658±30	182±20	150±40	4±3	622±55	734
Ni^{60}	8.8	53	843±40	185±20	75±30	5±3	728±55	754
Cu	8.8	53	866±20	215±10	89±20	5±3	735±30	756
Cu^{63}	8.7	53	860±40	213±20	104±20	5±3	746±50	748
Cu^{65}	8.7	53	905±50	220±20	55± 5	5±3	735±55	775
Zn	8.75	53	870±20	230±20	91±20	5±3	726±35	740
Ga	8.8	53	1040±30	260±50	50±50	5±3	825±75	745

The quoted energy bias allows for the non-linear response of NE102 scintillator [31]).

5. Results

The difference in the anticoincidence ratios for the target in and target out runs was combined with the difference due to the energy change in the defining counters to give a raw experimental cross section. Corrections were applied to this cross section for (1) energy unbalance between target and dummy, where applicable, (2) elastic scattering outside the stopping and antiscattering counters and (3) inelastic scattering into the counters above the bias levels.

The elastic scattering correction was obtained from refs. [14-24]): the scattering was integrated over the appropriate angular range and an interpolation made over energy. The inelastic scattering corrections were calculated from ref. [21]).

The raw experimental cross sections, the corrections applied and the final experimental cross section, together with the energy at the target centre, are given in table 1. This final cross section represents the total non-elastic reaction cross section; it differs from the optical model σ_R by the extent of any compound elastic involved and corresponds to $(\sigma_R - \sigma_{CE})$.

6. Discussion

The present results are in good agreement with the recent direct measurement of Wilkins [11]) and Bearpark [12]) and consistent with the (p, n) measurements of Albert [9]) and Wing [10]) combined with the (p, q) data of Hintz [3]). These five sets of measurements, using four different methods, give a value for copper significantly lower than the earlier measurements [4, 7, 8]) but a value which is still higher than predicted using an optical model with only volume absorption. The evidence for a surface absorption term, though less compelling than with the earlier results, is still strong.

When comparing the results with the predictions of the optical model, consideration must be given to the contributions due to compound elastic scattering which is not measured in the experiment. The extent of this contribution depends markedly on the number and type of channels open for decay of the compound nucleus. Near 10 MeV the most important competing channel is that for neutron decay via a (p, n) reaction. When the energy threshold for this reaction is low it becomes the principal mode of decay and the compound elastic contributions are small. This applies in all the cases considered here with the exception of Ni^{58}. Here the (p, n) threshold is 9.46 MeV and this channel is closed in the present work. The resulting relatively large compound elastic cross section for Ni^{58} at these energies has been estimated in a previous paper [14]) and corresponds to 40 ± 15 mb. This would make the reaction cross section for Ni^{58} 662 ± 57 mb. For the remaining experimental reaction cross sections of table 1, the compound elastic cross sections are most probably small in relation to the errors of the measurements †.

A set of optical model predictions (table 1) was computed using the potential found by Perey [25]) in his survey of differential cross section data, *viz*:

$$Vf_1(r) + i4a_2 W \frac{df_2(r)}{dr} + \boldsymbol{\sigma} \cdot \boldsymbol{l} \left(\frac{\hbar}{m_\pi c}\right)^2 \frac{1}{r} \frac{df_1}{dr} V_s,$$

$$f(r) = \left(1 + \exp \frac{r - R}{a}\right)^{-1}, \quad R_1 = R_2 = 1.25\, A^{\frac{1}{3}} \text{fm},$$

$$a_1 = 0.65 \text{ fm},$$

$$a_2 = 0.47 \text{ fm},$$

† Recent work [30]) at Birmingham suggests that Fe^{56} may also have a compound elastic cross section of the order of 40 mb.

$$V = 53.3 - 0.55E + \left[\frac{0.4Z}{A^{\frac{1}{3}}} + \frac{27(N-Z)}{A}\right] \quad \text{MeV},$$

$$W = 13.5 \quad \text{MeV},$$

$$V_s = 7.5 \quad \text{MeV}.$$

Of those targets studied here, only Al, Ni, Cu and Zn were used by Perey at the lowest energy considered (9.4 MeV). It is very noticeable that it is just these elements which give the best agreement between experiment and model in table 1. The agreement for V, Fe, Co and Ga is significantly less good and suggests that extrapolations from the regions used in determining the parameters should be treated with caution. The

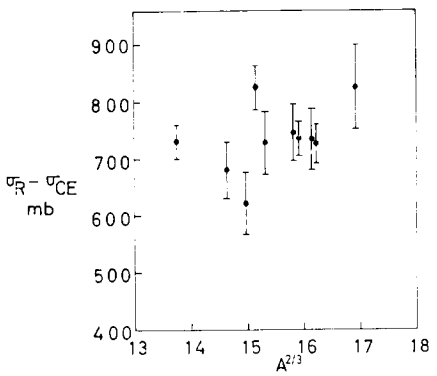

Fig. 4. The variation of $(\sigma_R - \sigma_{CE})$ with $A^{\frac{2}{3}}$ for $A = 51$ to 71. The dip near $A^{\frac{2}{3}} = 15$ (Ni^{58}) is removed if the σ_{CE} corrections are applied and σ_R plotted instead of $(\sigma_R - \sigma_{CE})$. These corrections raise the $A^{\frac{2}{3}} = 15$ point by 40 mb.

discrepancy for Co, where the experimental cross section is 59 mb higher than the model prediction, is particularly puzzling since both electron scattering experiments and analysis of elastic scattering differential cross sections and polarizations [14]) indicate the need for a radius lower than average.

Evidence for a dip in the reaction cross section for $Z = 28$ has been found for 40 MeV alphas [27]), 26.5 MeV deuterons [28]) and 29 MeV protons [29]). Such a dip was also suggested for 10 MeV protons in the results of Igo and Wilkins [11]) but was not conclusive because of uncertainties in the compound elastic contributions. In the present results (fig. 4), at 8.8 MeV, the existence of the dip relies very heavily on the Ni^{58} results; if this is corrected for the compound elastic contribution, $(40 \pm 15$ mb), it comes into closer agreement with the Ni^{60} result and the dip is less than the errors of measurement.

The separated isotope targets were prepared by the Atomic Energy Research Establishment, Harwell.

One of us (M.J.S.) wishes to thank the International Atomic Energy Agency and the Consejo Nacional de Investigaciones Cientificas (Argentina) for financial support.

References

1) A. E. Glassgold *et al.*, Phys. Rev. **106** (1957) 1207
2) J. S. Nodvik and D. S. Saxon, Phys. Rev. **117** (1960) 1539
3) V. Meyer and N. M. Hintz, Phys. Rev. Lett. **5** (1960) 209
4) G. W. Greenlees and O. N. Jarvis, Proc. Phys. Soc. **78** (1961) 1275
5) G. W. Greenlees and O. N. Jarvis, Proc. Kingston Conf. (1960)
6) B. R. Easlea, Proc. Phys. Soc. **78** (1961) 1285
7) K. F. Chackett, Proc. Phys. Soc. **80** (1962) 738
8) R. F. Carlson, R. M. Eisberg, R. H. Stokes and T. H. Short, Nuclear Physics **36** (1962) 511
9) R. D. Albert and L. F. Hansen, Phys. Rev. **123** (1961) 1749
10) J. Wing and J. R. Huizenga, Phys. Rev. **128** (1962) 280
11) B. D. Wilkins and G. Igo, Phys. Rev. **129** (1963) 2198
12) K. Bearpark, W. R. Graham and G. Jones, Int. Conf. on Nuclear Physics, Paris (June, 1964) C132
13) H. E. Conzett, Phys. Rev. **105** (1957) 1324
14) G. W. Greenlees *et al.*, Nuclear Physics **49** (1963) 496
15) W. F. Waldorf and N. S. Wall, Phys. Rev. **107** (1957) 1602
16) G. W. Greenlees, L. G. Kuo and M. Petravic, Proc. Roy. Soc. **A243** (1957) 206
17) B. W. Shore, N. S. Wall and J. W. Irvine, Phys. Rev. **123** (1961) 276
18) G. W. Greenlees, private communication (1964)
19) J. Benveniste, R. Booth and A. C. Mitchell, Phys. Rev. **123** (1961) 1818, **133** (1964) 217
20) K. Kikuchi, S. Yobayashi and K. Matsuda, J. Phys. Soc. Japan **14** (1959) 121
21) N. M. Hintz, private communication (1964)
22) C. Hu *et al.*, J. Phys. Soc. Japan **14** (1959) 861
23) C. A. Preskitt and W. P. Alford, Phys. Rev. **115** (1959) 389
24) A. K. Valter *et al.*, JETP **38** (1960) 1419
25) F. G. J. Perey, Phys. Rev. **131** (1963) 745
26) G. W. Greenlees and P. M. Rolph, Proc. Phys. Soc. **75** (1960) 201
27) G. Igo and B. D. Wilkins, Phys. Rev. **131** (1963) 1251
28) M. Sametband, to be published
29) M. Q. Makino, C. N. Waddell, R. M. Eisberg and J. Hestenes, Bull. Am. Phys. Soc. **8** (1963) 611
30) S. M. Scarrott, private communication
31) T. J. Gooding and H. G. Pugh, Nucl. Instr. **7** (1960) 189